https://doi.org/10.1016/j.atmosenv.2015.03.017

This is the Pre-Published Version.

Inhibition of the WNT/β-catenin pathway by fine particulate matter in haze: Roles of metals and polycyclic aromatic hydrocarbons

Kang-Yun Lee [a, b, 1], Jun-Ji Cao [c, 1], Chii-Hong Lee [d], Ta-Chih Hsiao [e], Chi-Tai Yeh [f], Thanh-Tuan Huynh [g], Yong-Ming Han [c], Xiang-Dong Li [h], Kai-Jen Chuang [i, j], Linwei Tian [k], Kin-Fai Ho [l, m, **], Hsiao-Chi Chuang [a, n, *]

[a] *Division of Pulmonary Medicine, Department of Internal Medicine, Shuang Ho Hospital, Taipei Medical University, Taipei, Taiwan*

[b] *Department of Internal Medicine, School of Medicine, College of Medicine, Taipei Medical University, Taipei, Taiwan*

[c] *Key Laboratory of Aerosol, SKLLQG, Institute of Earth Environment, Chinese Academy of Sciences, Xi'an 710075, China*

[d] *Department of Pathology, Shuang Ho Hospital, Taipei Medical University, Taipei, Taiwan*

[e] *Graduate Institute of Environmental Engineering, National Central University, Taoyuan, Taiwan*

[f] *Cancer Center, Shuang Ho Hospital, Taipei Medical University, Taipei, Taiwan*

[g] *Graduate Institute of Clinical Medicine, College of Medicine, Taipei Medical University, Taipei, Taiwan*

[h] *Department of the Civil and Environmental Engineering, The Hong Kong Polytechnic University, Kowloon, Hong Kong*

[i] *Department of Public Health, School of Medicine, College of Medicine, Taipei Medical University, Taipei, Taiwan*

[j] *School of Public Health, College of Public Health and Nutrition, Taipei Medical University, Taipei, Taiwan*

[k] *School of Public Health, The University of Hong Kong, Hong Kong SAR, China*

[l] *Jockey Club School of Public Health and Primary Care, The Chinese University of Hong Kong, Hong Kong*

[m] *Shenzhen Municipal Key Laboratory for Health Risk Analysis, Shenzhen Research Institute, The Chinese University of Hong Kong, Shenzhen, China*

[n] *School of Respiratory Therapy, College of Medicine, Taipei Medical University, Taipei, Taiwan*

© 2015. This manuscript version is made available under the CC-BY-NC-ND 4.0 license https://creativecommons.org/licenses/by-nc-nd/4.0/

* Corresponding author. Taiwan CardioPulmonary Research (T-CPR) Group, School of Respiratory Therapy, College of Medicine, Taipei Medical University, Taipei, Taiwan.

** Corresponding author. Jockey Club School of Public Health and Primary Care, The Chinese University of Hong Kong, Hong Kong, China.

ABSTRACT

Air pollution might have a great impact on pulmonary health, but biological evidence in response to particulate matter less than 2.5 μm in size ($PM_{2.5}$) has been lacking. Physicochemical characterization of haze $PM_{2.5}$ collected from Beijing, Xian and Hong Kong was performed. Biological pathways were identified by proteomic profiling in mouse lungs, suggesting that WNT/β-catenin is important in the response to haze $PM_{2.5}$. Suppression of β -catenin levels, activation of caspase-3 and alveolar destruction, as well as IL-6, TNF-α and IFN-γ production, were observed in the lungs. The inhibition of β -catenin, TCF4 and cyclin D1 was observed in vitro in response to haze $PM_{2.5}$. The inhibition of WNT/ β -catenin signaling, apoptosis-related results (caspase-3 and alveolar destruction), and inflammation, particularly including caspase-3 and alveolar destruction, were more highly associated with polycyclic aromatic hydrocarbons in haze $PM_{2.5}$. In conclusion, decreased WNT/ β -catenin expression modulated by haze $PM_{2.5}$ could be involved in alveolar destruction and inflammation during haze episodes.

INTRODUCTION

Rapid industrialization and urbanization in developing countries, such as China and the Southeast Asian countries, have led to an increase in air pollution. Particulate pollution is a serious environmental issue that is affecting air quality, climate and, in particular, human health (Institute, 2013). The 2010 Global Burden of Disease study reported that outdoor air pollution in the form of fine particles (≤2.5 μm in aerodynamic diameter; $PM_{2.5}$) is an important public health risk, contributing annually to 3.2 million premature deaths worldwide and 76 million years of healthy life lost (Murray et al., 2014). In China, the Global Burden of Disease analysis reported 1.2 million

premature deaths and 25 million healthy years of life lost in 2010, which were strongly associated with outdoor air pollution (Murray et al., 2014). Additionally, approximately 800 million people experienced an extremely severe and persistent haze pollution event at the beginning of 2013. However, the consequent health impact resulting from haze episodes remains unclear.

Haze is a weather phenomenon, mainly produced by combustion-derived pollutants, that leads to poor visibility because of the mixture of dust, moisture, smoke and vapor in the atmosphere (Sun et al., 2006b). Notably, epidemiological and clinical evidence has shown that haze pollutants contributed to 24% of respiratory admissions (Thurston et al., 1994) and a 30% increase in outpatient attendance (Emmanuel, 2000). The lung is the main portal of entry for aerial detritus, and as such, it is a critical organ for whole body defense by the clearance of depos- ited foreign materials. Alveolar epithelial cell apoptosis is an important step toward alveolar destruction in response to $PM_{2.5}$ (Farina et al., 2011). WNTsignaling has been reported to be a crucial mechanism controlling cell differentiation. The deregula- tion of WNT signaling regulates lung epithelial injury and repair processes (MacDonald et al., 2009). The central mediator of the WNT pathway is b-catenin, which is a transcription cofactor with T cell factor (TCF) and lymphoid enhancer factor (LEF) (Cadigan and Nusse, 1997). Libalova and colleagues (2012) suggested that exposure to $PM_{2.5}$ was related to WNT pathway expression in human embryonic lung fibroblasts (Libalova et al., 2012). However, little is known about the effects of WNT/b-catenin signaling in response to $PM_{2.5}$ exposure.

Haze occurs frequently in many cities in China, and it has been associated with pulmonary hospital admissions (Zhang et al., 2014). Xu and colleagues emphasized the importance of haze episodes in China (Xu et al., 2013), and the health impact of this type of pollution is an urgent issue in Asia. The respiratory system is a target organ for air pollutants, and short-term, high-

intensity exposure to haze $PM_{2.5}$ could cause distal lung injury. Here, we elucidated the potential proteomic-driven mechanisms in response to $PM_{2.5}$ exposure in a haze episode *in vivo*, and the WNT/β-catenin signaling pathway was examined *in vitro*. Additionally, the effects of metals and polycyclic aromatic hydrocarbons (PAHs) on the consequent bioreactivity were determined.

MATERIALS AND METHODS

Particle collection and physicochemical characterization

Two haze-influenced cities in China, Beijing (BJ) and Xian (XA), and one non-haze-influenced city, Hong Kong (HK), were selected to investigate the health effects caused by haze $PM_{2.5}$ exposure. $PM_{2.5}$ was collected for seven days during a haze air pollution episode from January 26, 2013, to February 1, 2013, using mini- volume samplers equipped with two $PM_{2.5}$ impactors operated at flow rates of 5 L/min (Airmetrics, USA). The $PM_{2.5}$ samples were collected onto 47-mm Teflon substrates for 24 h and were equilibrated in 50% ± 5% relative humidity to obtain their gravimetric mass concentrations.

Physicochemical characterization

One set of the $PM_{2.5}$ substrates was removed using two-stage sonication in methanol, followed by drying with a nitrogen stream. The samples were then resuspended in dimethyl sulfoxide (DMSO) (<0.01% vol in phosphate-buffered saline [PBS]) at 50 and 150 mg/mL. The hydrodynamic diameters of the $PM_{2.5}$ samples were determined using dynamic light scattering (DLS; Malvern Zetasizer Nano-ZS, Worcestershire, UK). The zeta potential of the samples was determined using a Zetasizer (Malvern Zetasizer Nano-ZS, Worcestershire, UK). The other set of the $PM_{2.5}$ substrates was analyzed by inductively coupled plasma-mass spectrometry (ICP-

MS) to identify 16 metals, according to our previous method: aluminum (Al), cesium (Cs), cadmium (Cd), cobalt (Co), copper (Cu), iron (Fe), nickel (Ni), lead (Pb), vanadium (V), zinc (Zn), chromium (Cr), manganese (Mn), molybdenum (Mo), selenium (Se), strontium (Se) and titanium (Ti) (Chuang et al., 2011a). The concentrations of 15 PAH compounds were reported previously (Lee et al., 2014).

Animals

The animal experiments were performed in accordance with the guidelines of the ethics review committee of the Laboratory Animal Center at Taipei Medical University, Taiwan (Approval No. LAC-101- 0003). Female six-week-old BALB/c mice were obtained from BiOLASCO (Taipei, Taiwan). The mice were provided free access to water and laboratory rodent chow. The mice's body weights were between 16 and 19 g during the experimental period. The mice were randomly divided into 7 groups (n = 6 per group), as shown in Fig. 1. On days 0 and 7, the mice in the exposure groups received an intratracheal instillation of 50 or 150 μg/kg of $PM_{2.5}$/mouse in PBS (<0.01% DMSO) under light anesthesia induced by isoflurane (Abbott Laboratories, Illinois, UK), whereas those in the control group received the same volume of vehicle PBS (<0.01% DMSO). On day 14, the animals were euthanized, and bronchoalveolar lavage fluid (BALF) and lung tissues were collected. The lung tissues were excised and snap-frozen or fixed in 4% (m/v) paraformaldehyde in PBS at 21 cm H_2O of pressure for histological analyses.

The doses applied in the present study were relevant for human exposure scenarios. The average $PM_{2.5}$ mass concentration for XA was 234 μg/m^3, which is equal to 1.4 μg/lung in humans (total lung capacity of 5.8 L for men). Considering the breathing frequency (30 times/min) and lung deposition rate (30%), the daily accumulative $PM_{2.5}$ is 17,589 μg/lung in humans, which is equal

to 3 μg/lung in the mouse (total lung capacity 0.001 L). Therefore, 50 μg/kg (equal to 1 μg/lung) and 150 μg/kg (equal to 2.9 μg/lung) were applied in the present study.

Protein extraction

For protein isolation, the lung tissue was homogenized in RIPA buffer (Sigma, MO, USA) with Complete™ protease inhibitor (Roche Diagnostics, Basel, Switzerland), according to the manufacturers' instructions.

Mass spectrometry and protein identification

Lung-isolated proteins were pooled from vehicle control and 150 μg/kg-exposed mice. The protein preparation was reported previously (Su et al., 2013). Briefly, the samples were denatured and reduced following digestion with trypsin (in 25 mM ammonium bicarbonate). Desalting of the samples were performed using C18 columns. A Thermo Q-Exactive mass spectrometer (Thermo Fisher Scientific, Bremen, Germany), coupled to an Ultimate 3000 RSLC system (Dionex, Sunnyvale, CA, USA), was used to analyze the tryptic peptides. A liquid chromatograph with C18 columns (Acclaim PepMap RSLC, 75 μm x 150 mm, 2 μm, Dionex) was used to separate peptides. The separation conditions were as follows (5% acetonitrile/0.1% formic acid for mobile phase A, 95% acetonitrile/ 0.1% formic acid for mobile phase B): linear gradient from 1% to 40% mobile phase B and then 40% - 90% mobile phase B. Five full MS scans (m/z) were performed, including 350-2000, 350-600, 600-800, 800-1200 and 1200-2000. The ten most intense ions from the MS scans were selected for MS/MS scans. The data were analyzed using Proteome Discoverer, version 1.3 for Mascot, data- base search software, with variable modifications for deamidation (NQ) and oxidation (M) and fixed modifications for

carbamidomethyl (C). The maximum mass tolerance was set to 10 ppm for precursor ions and to 0.05 Da for fragment ions. The maximum trypsin missed cleavage site was set to 2, and the filter threshold was set at 30 to guarantee a positive identification.

Protein function analyses

The Protein ANalysis THrough Evolutionary Relationships (PANTHER) classification system was used to determine the biological features of the identified proteins in the lung samples (Su et al., 2013). These proteins were analyzed against the *Mus musculus* reference dataset to summarize the functional annotations associated with individual genes/proteins or groups of genes/proteins. Biological processes, molecular functions and important pathways were presented.

ELISA

Enzyme-linked immunosorbent assay (ELISA) was used to determine b-catenin (Enzo, Lörrach, Germany) and caspase-3 activity (Millipore, Darmstadt, Germany) in lung-isolated proteins, according to the manufacturers' instructions.

Pulmonary inflammation

Interleukin 6 (IL-6), tumor necrosis factor α (TNF-α) and interferon γ (IFN-γ) concentrations in the BALF were assayed with BD Cytometric Bead Array tests (CA, USA), according to the manufacturer's instructions. Complexes of beads and the studied proteins labeled with phycoerythrin antibodies were acquired with a BD LSRFortessa™ cell analyzer (NJ, USA).

Imunohistochemistry

Immunohistochemistry (IHC) assays for β-catenin and caspase-3 expression were performed on sequential paraffin-embedded lung tissue sections. First, the tissue sections were deparaffinized and hydrated in sequential treatments of xylene, ethanol and water. Heat-mediated antigen retrieval in citrate buffer was performed before incubation with primary antibodies. Endogenous peroxidase activity and non-specific binding were blocked with 3% H_2O_2 and non-immune sera, respectively. Mouse monoclonal antibodies for b-catenin (dilution: 1:100) and caspase-3 (dilution: 1:2000) (Cell Signaling, MA, USA) were used. Biotinylated secondary antibodies and streptavidin-horseradish peroxidase (Maixin Biotechnology, Hong Kong) were added. The peroxidase reaction was developed with 3,3'-diaminobenzidine tetrahydrochloride (Maixin Biotechnology, Hong Kong). Light counterstaining was performed with hematoxylin, and the sections were dehydrated in alcohol prior to mounting. For the negative control, PBS was used in place of the primary antibodies.

Alveolar number analysis

The lung tissues were embedded in paraffin sections and then were stained with hematoxylin and eosin, according to standard protocols. For each mouse, 30 random fields of alveoli at 400x magnification (0.55 mm^2) were counted, and the average area of the alveoli was estimated. The histological samples were blindly examined under light microscopy by a histopathologist (CHL).

Cell culture and cell viability assays

Human alveolar epithelial A549 cells were obtained from the American Type Culture Collection (ATCC) and were cultured in RPMI 1640 medium (10% heat-inactivated fetal bovine serum and 1% penicillin-streptomycin antibiotics) at 37 ºC in a humidified atmosphere with 5% CO_2. Cells were grown to approximately 70e80% confluence following exposure to BJ, XA and HK $PM_{2.5}$ samples at increasing concentrations (0-100 μg/mL) for 24 h. Sulforhodamine B (SRB) colorimetric assay was used to determine the cell viability (Vichai and Kirtikara, 2006).

Western blotting

The cells were plated in six-well chamber slides (Nunc™, Thermo Fisher Scientific, MA, USA) for 24 h prior to exposure to 25 and 50 g/mL BJ and XA for an additional 24 h. The proteins isolated from lysed cells were subjected to sodium dodecyl sulfate poly- acrylamide gel electrophoresis (SDS-PAGE) and were electro- transferred onto polyvinylidene fluoride (PVDF) membranes (Millipore,Darmstadt, Germany). The primary antibodies for cyclin D1 (1:1000) and β-catenin (1:1000) were obtained from Cell Signaling. The antibodies for TCF4 (1:1000) and β-actin (1:1000) were obtained from Santa Cruz (Santa Cruz, CA, USA). Anti-mouse (1:5000) and anti-rabbit (1:2000) horseradish peroxidase (HRP)- conjugated secondary antibodies were obtained from Chemicon International (MA, USA). The blots were then blocked with 5% skim milk in PBST for 1 h and were probed with primary antibodies overnight at 4 ºC. Horseradish peroxidase-labeled secondary anti- body was then incubated for 60 min at room temperature and was washed with TBST. Enhanced chemiluminescence (ECL) western blotting reagents were used, followed by imaging using the Bio-Spectrum Imaging System (UVP, Upland, CA, USA).

Immunofluorescence

Fixation was performed in 2% paraformaldehyde and was permeabilized with 0.1% Triton X-100 in 0.01 M PBS (pH 7.4; containing 0.2% bovine serum albumin). Incubation with a rabbit polyclonal antibody against b-catenin, diluted 1:500 in PBS and containing 3% normal goat serum, was performed, whereas incubation with PBS served as a negative control. An anti-rabbit IgG FITC-conjugated secondary antibody (Jackson ImmunoResearch, PA, USA; 1:500 dilution) was incubated with the cells, following staining with 4',6-diamidino-2-phenylindole (DAPI). Microphotographs were ac- quired using an AxioCam MRc digital video camera and the Zeiss AxioVision software (Carl Zeiss, NY, USA).

Statistical analysis

Data are presented as the means ± standard deviations (SDs), and all of the experiments were conducted at least three times. For comparisons between groups, Student's *t*-test was used for the significance analysis. For comparisons among multiple values, one- way analysis of variance (ANOVA) with Tukey's post hoc test was used. Pearson's correlation coefficient was used to examine the correlation of β-catenin with caspase-3, alveolar number and inflammation (IL-6, TNF-α and IFN-γ) and the correlations of chemical compounds (metals and PAHs) with β-catenin, caspase-3, alveolar number and inflammation (IL-6, TNF-α and IFN-γ). For the correlations with chemicals, the relative bulk metals and PAH concentrations in the $PM_{2.5}$ (ng metals or PAHs/μg $PM_{2.5}$) were used. The statistical analyses were performed using GraphPad Version 5 for Microsoft Windows. The level of significance was set to $p < 0.05$.

RESULTS

Physicochemical characterization of haze $PM_{2.5}$

Table 1 summarizes the meteorological conditions and physical and metal characteristics of the $PM_{2.5}$ samples. The humidity (%) of BJ, XA and HK were 77 ± 15, 48 ± 17 and 73 ± 6, respectively. The visibility (m) of BJ and XA were 3353 ± 2949 and 2130 ± 1503, respectively. The hydrodynamic diameters of the BJ, XA and HK $PM_{2.5}$ were 207e253 nm at 50 μg/mL and 422-466 nm at 150 μg/mL. The zeta potential values for these samples were between -14 and -34 at 50 μg/mL and between -7 and -18 at 150 μg/mL. The XA $PM_{2.5}$ sample had the highest metal concentration (3318.0 ± 1280.9 ng/m^3), whereas the HK $PM_{2.5}$ had the lowest metal concentration (570.2 ± 99.3 ng/m^3). Al, Fe and Zn were the most abundant metallic elements among the BJ, XA and HK samples.

Proteomic profiling in lung tissue and functional analyses

The overlaps in the protein profiles between the vehicle control (979 proteins) and the BJ (903 proteins), XA (937 proteins) and HK (977 proteins) $PM_{2.5}$ exposure groups were determined (Fig. 2a). In total, 130, 163 and 176 unique proteins for BJ, XA and HK $PM_{2.5}$ were discovered, respectively, whereas 206, 205 and 178 unique proteins for the control after exposure to BJ, XA and HK$PM_{2.5}$, respectively, were discovered. The details of the unique proteins are provided in Supplementary Information Tables S1 and S2. There were 40 unique proteins among BJ, XA and HK $PM_{2.5}$, which are presented in Supplementary Information Table S3. The haze-specific proteins were associated with 17 biological processes (Fig. 2b): cell communication, cellular processes, localization, transport, cellular component organization, apoptosis, system processes, reproduction, response to stimuli, regulation of biological processes, homeostatic processes, developmental processes, generation of precursor metabolites and energy, metabolic processes, the cell cycle, immune system processes and cell adhesion. Cell communication (9% for BJ, 14%

for XA and 12% for HK), cellular processes (16% for BJ, 20% for XA and 18% for HK) and metabolic processes (22% for BJ, 20% for XA and 20% for HK) were the critical biological processes that were modulated in response to haze exposure. Furthermore, 10 molecular functions were identified (Fig. 2b): ion channel activity, transporter activity, translation regulatory activity, transcription regulatory activity, enzyme regulatory activity, cata- lytic activity, receptor activity, structural molecular activity, binding and motor activity. Catalytic activity (34% for BJ, 30% for XA and 29% for HK), structural molecular activity (14% for BJ, 15% for XA and 12% for HK) and binding activity (31% for BJ, 35% for XA and 40% for HK) were the critical molecular functions that were modulated in response to haze exposure.

The control-specific proteins were associated with 12 biological processes (Fig. 2c): cellular component organization or biogenesis, cellular processes, localization, apoptotic processes, reproduction, biological regulation, response to stimulus, developmental pro- cesses, multicellular organismal processes, biological adhesion, metabolic processes and immune system processes. Cell communication (18% for BJ, 16% for XA and 17% for HK), localization (11% for BJ, 10% for XA and 12% for HK) and metabolic processes (36% for BJ, 38% for XA and 36% for HK) were the critical biological processes in the control group that were modulated in response to haze expo- sure. Furthermore, 10 molecular functions were identified (Fig. 2c): transporter activity, translation regulator activity, protein binding transcription factor activity, enzyme regulator activity, catalytic activity, receptor activity, nucleic acid binding transcription factor activity, antioxidant activity, structural molecule activity and binding. Catalytic activity (34% for BJ, 36% for XA and 38% for HK), structural molecular activity (12% for BJ, 10% for XA and 9% for HK) and binding activity (33% for BJ, 33% for XA and 31% for HK) were the critical molecular functions in the control groups that were modulated in response to haze exposure.

The haze-specific proteins in BJ, XA and HK were mainly involved in 17 pathways (Fig. 2b), including those mediating 5-hydroxytryptamine degradation, blood coagulation, cadherin signaling, cytoskeletal regulation by Rho GTPases, EGF receptor signaling, FGF signaling, heterotrimeric G-protein signaling via Gq alpha and Go alpha, heterotrimeric G-protein signaling via rod outer segment phototransduction, Huntington disease, chemokine- and cytokine-mediated inflammation, integrin signaling, interleukin signaling, ionotropic glutamate receptor signaling, nicotinic acetylcholine receptor signaling, PDGF signaling, ubiquitin protea- some signaling and WNT signaling. Notably, the WNT signaling pathway (6% for BJ, 7% for XA and 7% for HK) was identified as a critical pathway modulated in response to haze exposure.

Twenty pathways (>2%) identified in the control-specific proteins in response to BJ, XA and HK (Fig. 2c), including those mediating the muscarinic acetylcholine receptor 2 and 4 signaling pathway, inflammation mediated by the chemokine and cytokine signaling pathway, the interferon-gamma signaling pathway, Parkinson disease, the metabotropic glutamate receptor group II pathway, GABA-B receptor II signaling, the heterotrimeric G-protein signaling pathway-Gi alpha- and Gs alpha-mediated pathway, the interleukin signaling pathway, the EGF receptor signaling integrin signaling pathway, de novo purine biosynthesis, the cadherin signaling pathway, the Ras pathway, the WNT signaling pathway, angiogenesis, the gonadotropin-releasing hormone receptor pathway, the FGF signaling pathway and the ubiquitin proteasome pathway. Notably, the WNT signaling pathway (3% for BJ, XA and HK) was identified as a critical pathway modulated in response to haze exposure.

Suppression of β-catenin

At 150 μg/mL, the BJ and XA haze $PM_{2.5}$ significantly suppressed b-catenin expression by 0.6-

fold and 0.7-fold, respectively, compared with the control ($p < 0.05$) (Fig. 3a). Consistently, IHC analyses of the lung sections, obtained after exposure to 150 μg/mL haze $PM_{2.5}$, showed a reduction of β-catenin in the lung, particularly in the BJ and XA samples.

Alterations in lung caspase-3 activity and alveolar numbers

At 150 μg/mL, the BJ, XA and HK haze $PM_{2.5}$ samples significantly stimulated caspase-3 activity by 2.5-, 2.1- and 1.7-fold, respectively, compared with the control ($p < 0.05$) (Fig. 3b). Consistently, IHC analyses of the lung sections, obtained after exposure to 150 μg/mL haze $PM_{2.5}$, showed increased caspase-3 in the lung. To assess further the changes in the alveolar structure resulting from apoptosis in response to haze $PM_{2.5}$ exposure, the alveolar numbers in the lung sections were examined (Fig. 3c). The alveolar number significantly decreased after exposure to BJ $PM_{2.5}$ compared with the control ($p < 0.05$) in a dose-dependent manner. This finding was in agreement with the histological analyses of the lung sections, which revealed that BJ $PM_{2.5}$ exposure caused more alveolar destruction than the other $PM_{2.5}$ samples. HK $PM_{2.5}$ exposure caused more interstitial inflammatory cell infiltration into the alveolar space. The correlations of b-catenin with caspase-3 activity and alveolar number were resolved using Pearson's correlation. β-catenin was negatively correlated with caspase-3 activity ($r = -0.9468$, $p < 0.05$) (Fig. 3d), whereas β-catenin was positively correlated with alveolar number ($r = 0.8156$, $p < 0.05$).

Association of metals and PAHs with β-catenin caspase-3 activity and alveolar numbers

The correlations of the chemical compounds (metals and PAHs) of the haze $PM_{2.5}$ to β-catenin, caspase-3 activity and alveolar numbers are shown in Fig. 3e. There were no correlations

observed between the total metals and β-catenin ($r = -0.6673$, $p = 0.1476$), caspase-3 activity ($r = 0.6872$, $p = 0.1314$) or alveolar numbers ($r = -0.3345$, $p = 0.5170$). The total PAHs were significantly correlated with b-catenin ($r = -0.8431$, $p < 0.05$), caspase-3 activity ($r = 0.9272$, $p < 0.05$) and alveolar numbers ($r = -0.9483$, $p < 0.05$). We further examined the correlation of individual metals and PAHs with β-catenin, caspase-3 activity and alveolar number (Table 2). β- catenin was correlated with Cd ($r = -0.8607$, $p < 0.05$), Pb ($r = -0.8893$, $p < 0.05$), Cr ($r = -5396$, $p < 0.05$), Mn ($r = -0.9539$, $p < 0.05$), Mo ($r = -0.8197$, $p < 0.05$) and Se ($r = -0.8383$, $p < 0.05$). Caspase-3 activity was correlated with Cd ($r = 0.9463$, $p < 0.05$), Fe ($r = 0.8119$, $p < 0.05$), Pb ($r = 0.9640$, $p < 0.05$), Mn ($r = 0.9651$, $p < 0.05$), Mo ($r = 0.8911$, $p < 0.05$) and Se ($r = 0.8609$, $p < 0.05$). Alveolar number was correlated with Cd ($r = -0.8860$, $p < 0.05$) and Pb ($r = -0.9561$, $p < 0.05$). Regarding the PAHs, β-catenin was correlated with chrysene ($r = -0.7910$, $p < 0.05$), benzo(bþk)fluoranthene ($r = -0.8206$, $p < 0.05$) and benzo(a)pyrene ($r = -0.8505$, $p < 0.05$). Caspase-3 activity was correlated with naphthalene ($r = 0.8144$, $p < 0.05$), acenaphthylene ($r = 0.8125$, $p < 0.05$), acenaphthene ($r = 0.8284$, $p < 0.05$), phenanthrene ($r = 0.8333$, $p < 0.05$), anthracene ($r = 0.8230$, $p < 0.05$), fluoranthene ($r = 0.8428$, $p < 0.05$), pyrene ($r = 0.8845$, $p < 0.05$), benz(a)anthracene ($r = 0.8487$, $p < 0.05$), chrysene ($r = 0.8780$, $p < 0.05$), benzo(bþk)fluoranthene ($r = 0.9090$, $p < 0.05$), benzo(a) pyrene ($r = 0.9368$, $p < 0.05$), indeno(1,2,3-cd)pyrene ($r = 0.9144$, $p < 0.05$) and benzo(g,h,i)perylene ($r = 0.8575$, $p < 0.05$). Alveolar number was correlated with naphthalene ($r = -0.8743$, $p < 0.05$), acenaphthylene ($r = -0.8699$, $p < 0.05$), acenaphthene ($r = -0.9272$, $p < 0.05$), phenanthrene ($r = -0.9480$, $p < 0.05$), anthracene ($r = -0.9419$, $p < 0.05$), fluoranthene ($r = -0.9526$, $p < 0.05$), pyrene ($r = -0.9597$, $p < 0.05$), benz(a)anthracene ($r = -0.9477$, $p < 0.05$), chrysene ($r = -0.9412$, $p < 0.05$),

benzo(bþk)fluoranthene ($r = -0.9263$, $p < 0.05$) and benzo(a) pyrene ($r = -0.9230$, $p < 0.05$).

Pulmonary inflammation

Haze $PM_{2.5}$ exposure in the lungs led to increased production of IL-6, TNF-α and IFN-γ compared with the control ($p < 0.05$; Fig. 4a), as determined in the BALF, and this increase was particularly evident in the BJ $PM_{2.5}$ sample. Pulmonary exposure to haze $PM_{2.5}$ led to significantly increased IL-6 production in the BALF samples ($p < 0.05$) in a dose-dependent manner, particularly for the BJ sample. The TNF-a and IFN-g concentrations were significantly increased post-haze $PM_{2.5}$ exposure ($p < 0.05$), but dose-dependent responses were only observed in the BJ (TNF-α in BALF and IFN-γ) and XA $PM_{2.5}$ samples (IFN-γ). The correlations of β-catenin with IL- 6, TNF-a and IFN-g were examined using Pearson's correlation (Fig. 4b), resulting in r values of -0.7778 for IL-6 ($p < 0.05$), -0.7253 for TNF-α ($p = 0.0651$) and -0.5143 for IFN-γ ($p = 0.2376$). IL-6 was negatively correlated with β-catenin.

Association of metals and PAHs with pulmonary inflammation

Fig. 4c shows the correlations of the metals and PAHs with IL-6, TNF-α and IFN-γ. No correlations were observed between the total metals and IL-6 ($r = 0.3298$, $p = 0.5233$), TNF-α ($r = 0.3090$, $p = 0.5513$) or IFN-γ ($r = 0.1226$, $p = 0.8170$). The total PAHs were significantly correlated with IL-6 ($r = 0.9324$, $p < 0.05$), TNF-α ($r = 0.9341$, $p < 0.05$) and IFN-γ ($r = 0.8483$, $p < 0.05$).

Decrease in cell viability

A significant dose-dependent reduction in cell viability was observed in response to BJ, XA and HK $PM_{2.5}$ (Fig. 5a). Cell viability displayed the greatest reduction in response to the BJ samples, followed by the XA samples and then the HK samples, with half- maximal inhibitory concentrations (IC-50) of 58.33 μg/mL, 67.83 μg /mL and 76.05 μg /mL, respectively.

Suppression of WNT/β-catenin expression

β-catenin expression was suppressed by 70% (for BJ at 50 μg/mL) and 60% (for XA at 50 μg/mL), and it was significantly reduced in the nuclei following BJ exposure, compared with the control (Fig. 5b). The WNT signaling transducer T cell transcription factor-4 (TCF4) was decreased by 60% (for BJ at 50 μg/mL) and 50% (for XA at 50 μg/ mL). Consequently, the expression of cyclin D1, which is a down- stream molecule of b-catenin signaling, was down-regulated by 60% (for BJ at 50 μg/mL) and 40% (for XA at 50 μg/mL). The potential associations of the total metals and PAHs with β-catenin were further investigated (Fig. 5c). We observed a β-catenin inhibition trend among the total metals and PAHs, showing that the chemicals could be negatively associated with β-catenin regulation in the $PM_{2.5}$ samples.

DISCUSSION

Air pollution is a worldwide public health issue, particularly in areas affected by rapid population growth and economic development, and it has been suggested to be an important contributor to cardiopulmonary morbidity and mortality. For example, pulmonary exposure to particulate pollutants resulted in airway remodeling, which could be component-specific (Churg and Wright, 2002). However, the mechanisms underlying acute exposure to high levels of $PM_{2.5}$ (such as those encountered during haze episodes) remain unclear. Additionally, the component-specific health effects caused by haze $PM_{2.5}$ remain poorly understood. Here, we took a comprehensive approach to discovering the pulmonary effects of haze $PM_{2.5}$ exposure via proteomic expression, biological analyses, pathological analyses and WNT/β-catenin expression *in vivo*, as well as a confirmation in an *in vitro* study. The major findings of the

present study were that haze $PM_{2.5}$ resulted in significant sup- pression of WNT/β-catenin signaling *in vivo* and *in vitro*. Apoptosis, alveolar destruction and inflammation in the lungs were significantly caused by haze $PM_{2.5}$. The inhibition of WNT/β-catenin signaling, the apoptosis-related results (caspase-3 and alveolar destruction) and inflammation were associated with the PAHs in $PM_{2.5}$.

To achieve the aims of this study, $PM_{2.5}$ was collected from two severely haze-influenced cities, BJ and XA, and a control city, HK, during a haze episode. The $PM_{2.5}$ mass concentrations in the haze- affected cities were significantly higher than the World Health Organization (WHO) air quality guideline for daily average $PM_{2.5}$ exposure (25 μg /m^3) (WHO, 2006). Our previous report showed that the haze $PM_{2.5}$ mass concentrations in BJ and XA were 8.8 times and 9.4 times greater, respectively, than the WHO $PM_{2.5}$ daily average (Lee et al., 2014). Consistently, previous studies have shown that $PM_{2.5}$ mass concentrations in BJ have reached 242 mg/m^3 (Sun et al., 2006b), and a major proportion of haze episode particles consists of respirable $PM_{2.5}$ (Sun et al., 2013). Tian and colleagues (2014) observed that secondary organic matter and inorganic aerosols were accounted for 26% and 36% of $PM_{2.5}$, respectively, during a haze episode (Tian et al., 2014). This finding suggests that the characterization of chemical profiles is a key step in under- standing the potential health impacts of haze $PM_{2.5}$. We previously showed that four- and five-ring PAHs predominated in haze $PM_{2.5}$ (Lee et al., 2014). The total PAH level in the BJ $PM_{2.5}$ was 1.3-fold higher than the XA $PM_{2.5}$ and 23.1-fold higher than the HK $PM_{2.5}$. In the present study, we further demonstrated that the total metal in the XA $PM_{2.5}$ was 1.2-fold higher than the BJ $PM_{2.5}$ and 5.8-fold higher than the HK $PM_{2.5}$. In addition, Al, Fe, Pb and Zn were distinct metal components of the BJ and XA particles, compared with the $PM_{2.5}$ collected in HK. These organic and inorganic com- pounds have been linked to the particle toxicity; however, the pulmonary impacts caused

by haze $PM_{2.5}$ remain unclear.

A mouse model was used to investigate the potential mechanisms in the context of haze $PM_{2.5}$ stress. To discover the potential health effects in response to haze $PM_{2.5}$, the proteomic approach was applied. We showed that the majority of uniquely identified proteins after haze $PM_{2.5}$ exposure involved the WNT signaling pathway, encompassing all of the functional categories of the pathway, and they were expressed in the lung tissues following exposure to haze $PM_{2.5}$ from the three aforementioned cities. Wang and colleagues (2011) used microarrays to assess gene expression in the small airway epithelium, obtained via bronchoscopy and brushing of non-smokers and smokers among healthy and pulmonary disease subjects (Wang et al., 2011). These researchers showed that the down-regulation of WNT signaling was a critical pathway in the differentiation of epithelial tissues. Based on these data, we suspected that the WNT/β-catenin pathway plays an important role in the response to haze $PM_{2.5}$ in the lung environment. Following haze $PM_{2.5}$ exposure, the expression of the WNT mediator β-catenin was decreased in lung tissue, suggesting that β-catenin expression was suppressed in a dose-dependent manner. In the adult human lung, the WNT pathway is an important regulator of cell fate decisions and lung cell differentiation (Nelson and Nusse, 2004). To understand the effects of haze $PM_{2.5}$ on lung cell viability, caspase-3 activity was determined in murine lungs. We observed significant apoptotic activation of caspase-3 in the lung tissue in response to haze $PM_{2.5}$, demonstrating the destruction of alveolar structures by decreasing alveolar numbers. This pathological finding was caused by airspace enlargement. Cell apoptosis and alveolar destruction were significantly correlated with β-catenin alterations; this finding suggested that β-catenin was sup- pressed by haze $PM_{2.5}$, leading to alveolar airspace enlargement. Lam and colleagues (2011) demonstrated that WNT down-regulation occurred rapidly when airspace enlargement was evident, mostly occurring within 1

day after injury and remaining low for 1 - 2 weeks (Lam et al., 2011), which is in accordance with our results. After exposure to haze $PM_{2.5}$, the efforts of the lung to repair or reverse the damage might be suppressed or absent; therefore, investigation of the WNT/β-catenin pathways in response to haze $PM_{2.5}$ is required.

Furthermore, we showed that inflammatory responses were triggered by haze $PM_{2.5}$ exposure. Inflammatory cytokines were shown to retard epithelial cell proliferation through inhibition of the β-catenin/TCF pathway (Capaldo et al., 2012). These results supported our finding of a negative correlation between β-catenin expression and IL-6 production. Taken together, our findings indicated that pulmonary exposure to haze $PM_{2.5}$ involved WNT/β-catenin signaling for the repair and regeneration phases after lung injury.

Following our initial observation, we determined whether WNT/ β-catenin activation represented an important mechanism in response to haze $PM_{2.5}$ exposure. WNT/ β-catenin expression is highly regulated by haze $PM_{2.5}$, and different WNT regulators and inhibitors have been previously described (Chilosi et al., 2003; Konigshoff and Eickelberg, 2010). To evaluate further the effects of haze $PM_{2.5}$ on WNT/ β-catenin signaling, we performed a detailed analysis of the WNT/ β-catenin pathway *in vitro*. Because of the relative smaller amount of $PM_{2.5}$ in HK during the haze episode, only the BJ and XA samples were further studied *in vitro*. β-catenin expression was suppressed by haze $PM_{2.5}$ in A549 cells, in accordance with the results in mouse lungs. The WNT-mediated cell fate has been reported to be dependent on the activation of β-catenin/ TCF transcription (Li et al., 2012). Caspase-3 is an important regulator for apoptotic signals from initiator caspases in an apoptotic pathway, which has been connected to WNT/β-catenin pathway. For example, caspase-dependent WNT/β-catenin induced apoptosis was supported by the result form experiment using caspase inhibitor and WNT inhibitor in macrophages

(Wu et al., 2014). A previous study further showed that β-catenin was proteolytically cleaved by caspase-3 during apoptosis (Steinhusen et al., 2000). Inhibition of β-catenin and TCF blocked WNT- regulated cell survival and increased the cells sensitivity to apoptotic stimuli. Cyclin D1, the downstream molecule of β-catenin signaling, plays an important role in the regulation of proliferation and the cell cycle (Yang et al., 2006). Imoto and colleagues (1998) observed that the inhibition of cyclin D1 expression induced apoptosis (Imoto et al., 1998). Our results demonstrated that exposure to haze $PM_{2.5}$ resulted in the down-regulation of the WNT/β-catenin pathway and suppression of β-catenin in mouse lung tissues. Importantly, a reduction in WNT/β-catenin signaling was observed *in vitro*, which was further confirmed by the sup- pression of β-catenin in mouse lung tissues following exposure to haze $PM_{2.5}$. The *in vivo* and *in vitro* results suggested that the reduced activity of WNT/β-catenin signaling is an important mechanism in response to haze $PM_{2.5}$ exposure.

Compound-specific effects in reaction to particle toxicity are important issues that must be clarified. Metals and PAHs, the pre- dominant constituents in haze $PM_{2.5}$ (Tian et al., 2014) and recognized toxic agents (Chuang et al., 2012, 2011b), were correlated with β-catenin, caspase-3, alveolar number and inflammation. Importantly, we observed that PAHs were more highly associated with β-catenin inhibition, caspase-3 production, alveolar destruction and inflammation than metals were, particularly for caspase-3 and alveolar number. Fairbairn and colleagues (2012) found that PAHs disrupted β-catenin signaling in zebrafish embryos (Fairbairn et al., 2012). Our findings were also supported by a previous study that found that apoptosis, airway enlargement and inflammation were induced by exposure to coal dust and PAHs (Ghanem et al., 2006). Hydroxyl derivatives are converted from PAHs by cytochrome P450, epoxide hydrolase and dihydrodiol dehydrogenase (Xia et al., 2004), leading to oxidative imbalance and DNA adduction

(Sun et al., 2006a). The mechanisms underlying the interactions between WNT/β-catenin and PAHs require further investigation. The BJ $PM_{2.5}$ had higher PAH concentrations than XA and HK did, which is inconsistent with the alteration in β-catenin, caspase-3 and alveolar number in response to the haze $PM_{2.5}$. However, previous reports have shown that metals in particles, particularly the water-soluble fraction, can induce apoptosis and inflammation (Huang et al., 2004). The difference may be caused by the methanol extraction method of removing particles from the filters used in the present study. Further investigations are necessary to investigate the associations of β-catenin inhibition, caspase- 3 production and alveolar destruction with metals.

CONCLUSION

In conclusion, we demonstrated an association between the pulmonary exposure to haze particulate pollution and adverse human health regulation through suppression of the WNT/b-catenin pathway. The health impacts on the respiratory system could be associated with the chemical characteristics of particulate pollution during haze episodes, particularly PAHs. A more informative method for proteomics should be applied for environmental toxicology in future studies, such as iTRAQ equipped with LC-MS/ MS. The results of the present study could close the gaps be- tween epidemiological and clinical research and could demonstrate the possibility that PAHs in haze PM2.5 can disrupt WNT/b-catenin signaling, leading to apoptosis, alveolar destruction and inflammation.

FUNDING

This study was founded by the Ministry of Science and Tech- nology of Taiwan (MOST103-2314-B-038-018), the Research Grants Council of the Hong Kong Special Administrative Region China (Project

No. CUHK 412612), the National Natural Science Founda- tion of China (41230641) and the Strategic Priority Research Pro- gram of the Chinese Academy of Science (XDA05100401).

ACKNOWLEDGMENTS

The authors wish to thank Miss Yi-Syuan Lin for the technical assistance of this research.

SUPPLEMENTARY DATA

Supplementary data related to this article can be found at http://dx.doi.org/10.1016/j.atmosenv.2015.03.017.

FIGURES AND TABLES

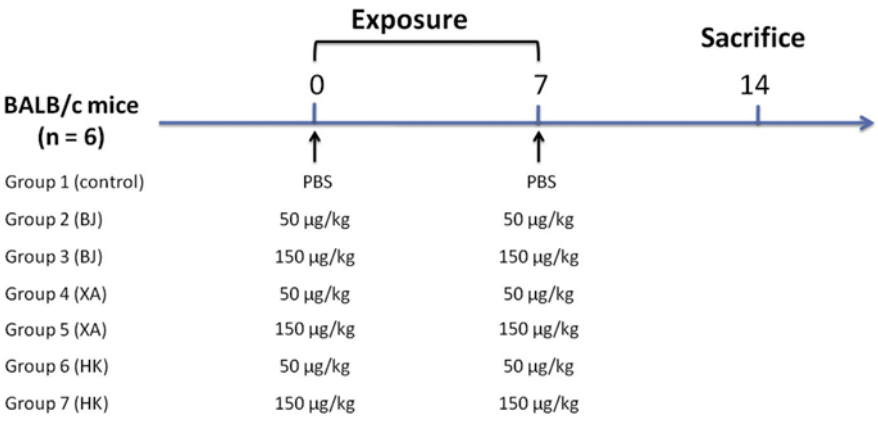

Fig. 1. Experimental design for investigating the pulmonary effects of $PM_{2.5}$ collected from BJ, XA and HK during a haze episode.

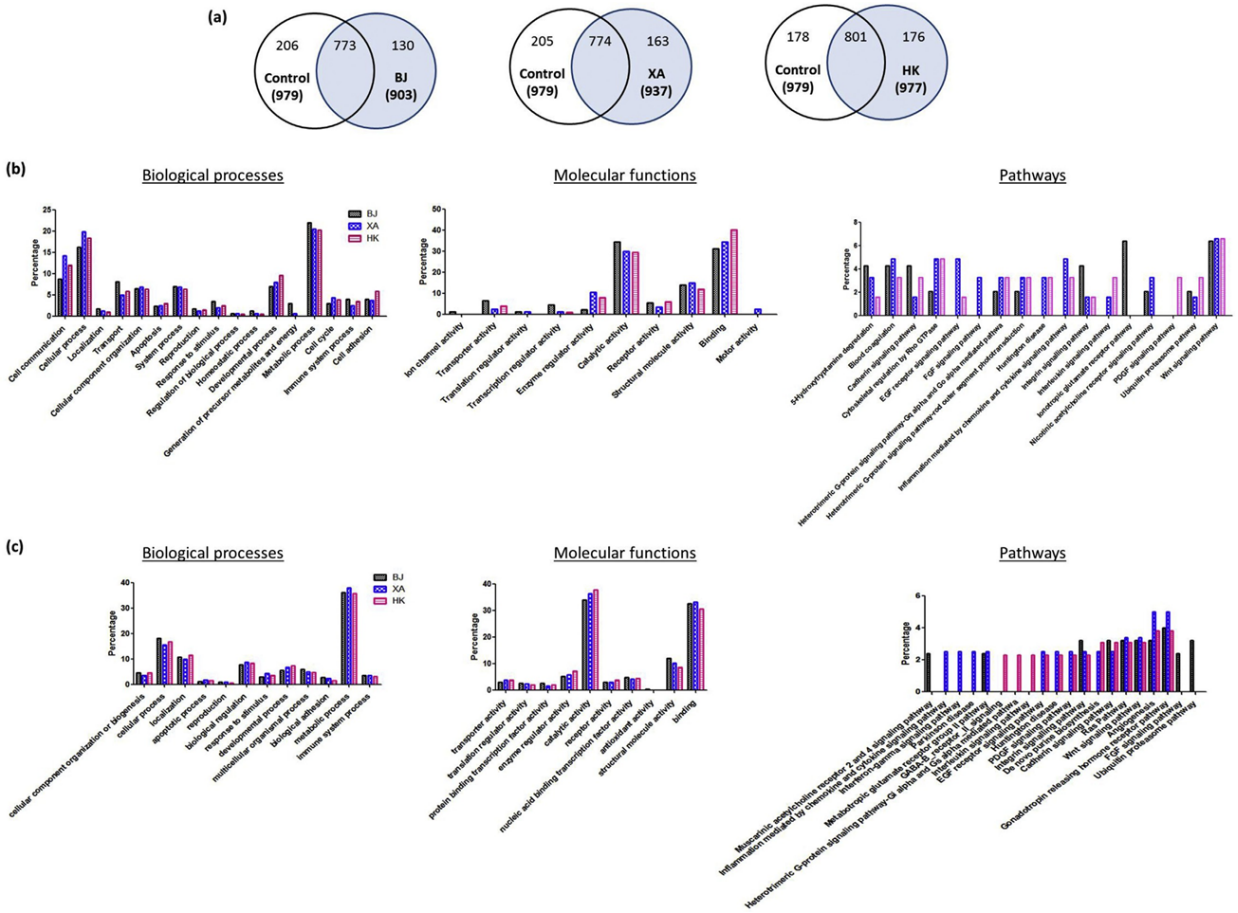

Fig. 2. (a) Venn diagram showing the lung proteins in common between or unique to the controls and BJ, XA or HK $PM_{2.5}$ exposure. (b) Biological processes, molecular functions and pathways associated with haze-specific proteins were determined using PANTHER analysis. (c) Biological processes, molecular functions and pathways in the control associated with control-specific proteins were determined using PANTHER analysis. The WNT signaling pathway was identified as a critical pathway modulated in response to haze exposure.

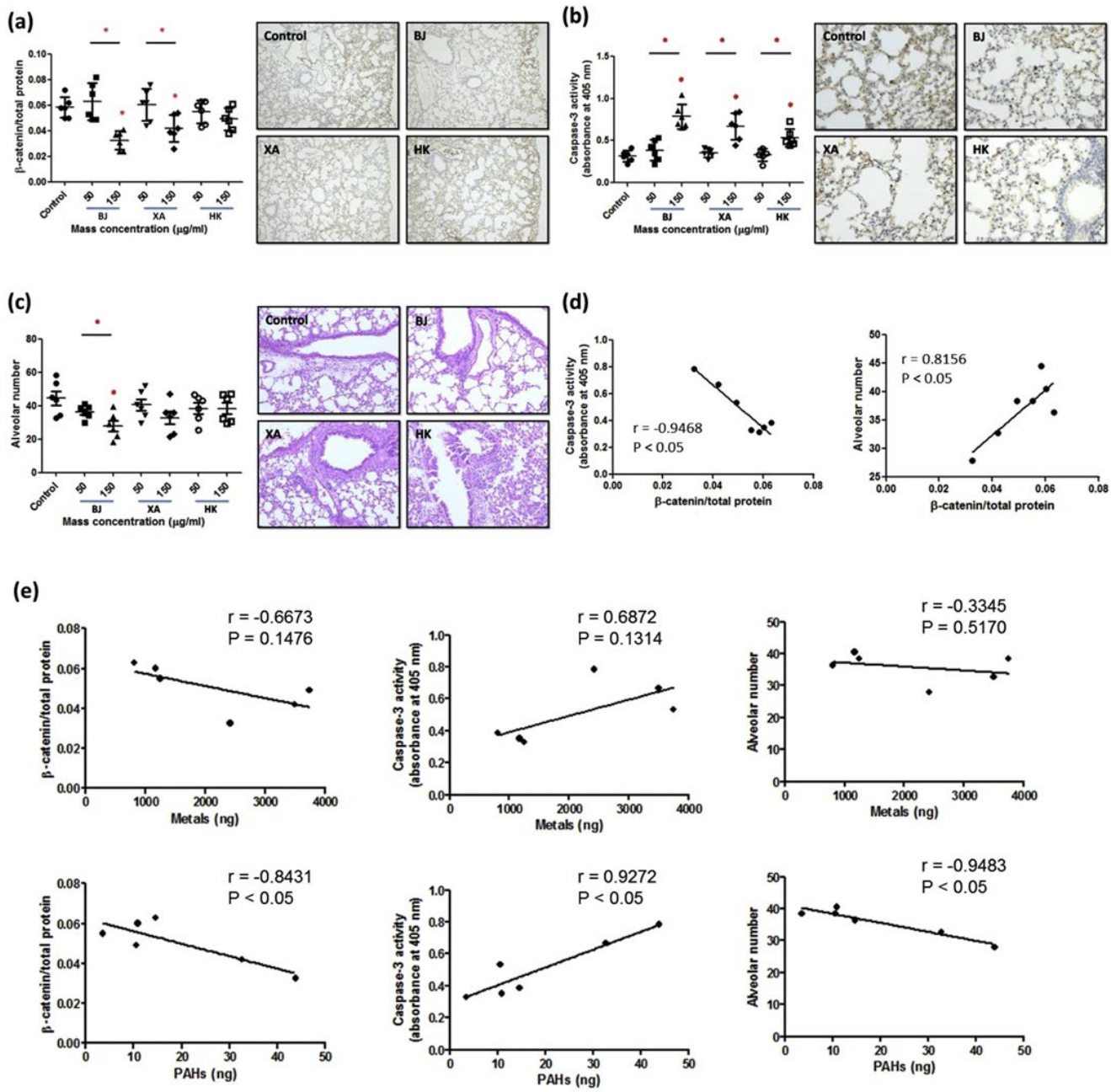

Fig. 3. Effects of haze $PM_{2.5}$ (BJ, XA and HK) on (a) β-catenin, (b) caspase-3 activity and (c) alveolar number in mouse lungs. (d) Associations between β-catenin and caspase-3 activity or alveolar number were determined by Pearson's correlation coefficient. (e) Associations of β-catenin, caspase-3 activity and alveolar number with total metals and PAHs were determined by Pearson's correlation coefficient. *$p < 0.05$.

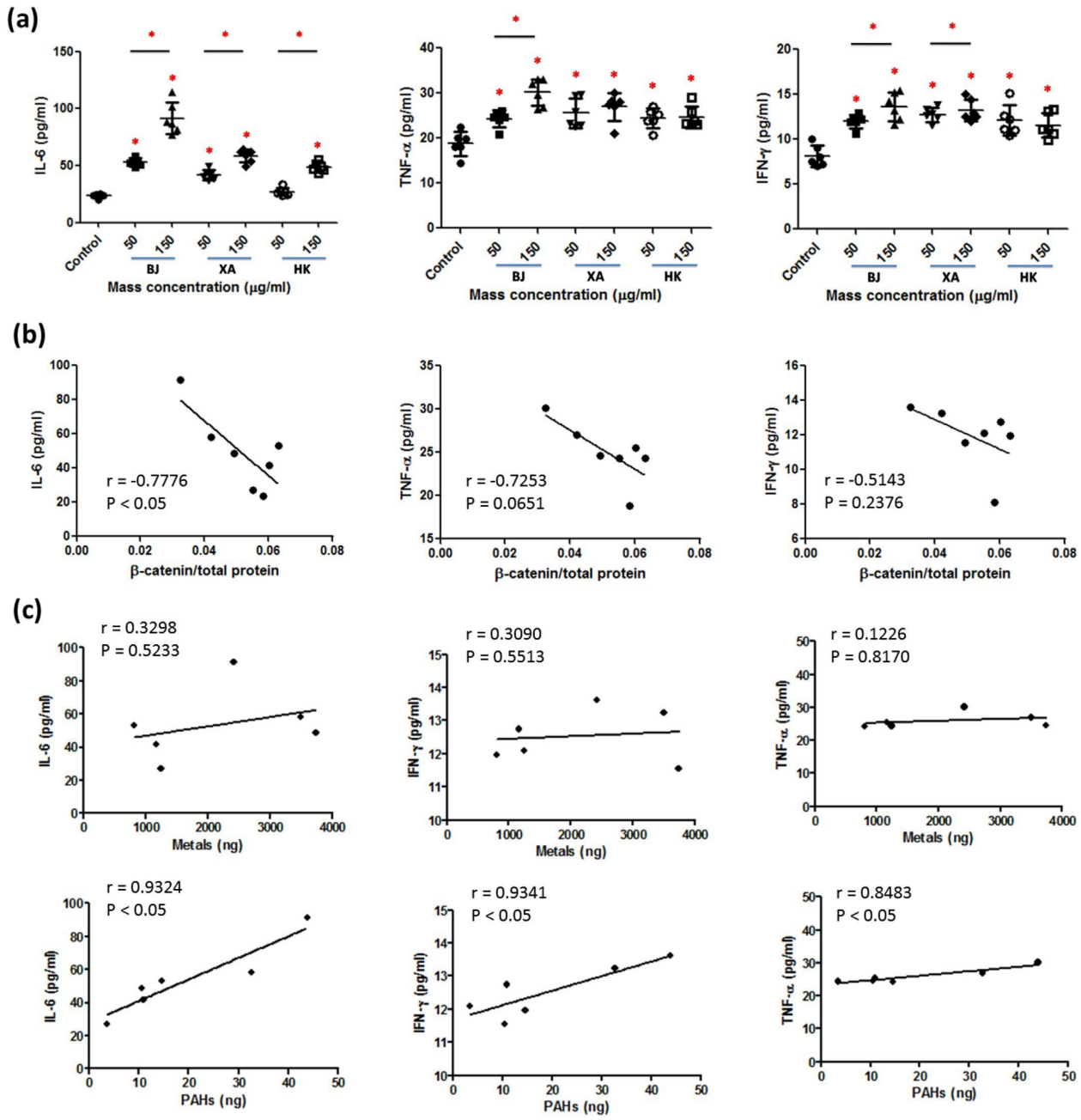

Fig. 4. (a) Effects of haze $PM_{2.5}$ (BJ, XA and HK) on IL-6, TNF-α and IFN-γ in the BALF and plasma post-exposure. (b) Associations between β-catenin and IL-6, TNF-α or IFN-γ were determined by Pearson's correlation coefficient. (c) Associations of IL-6, TNF-α and IFN-γ with total metals and PAHs were determined by Pearson's correlation coefficient. *$p < 0.05$.

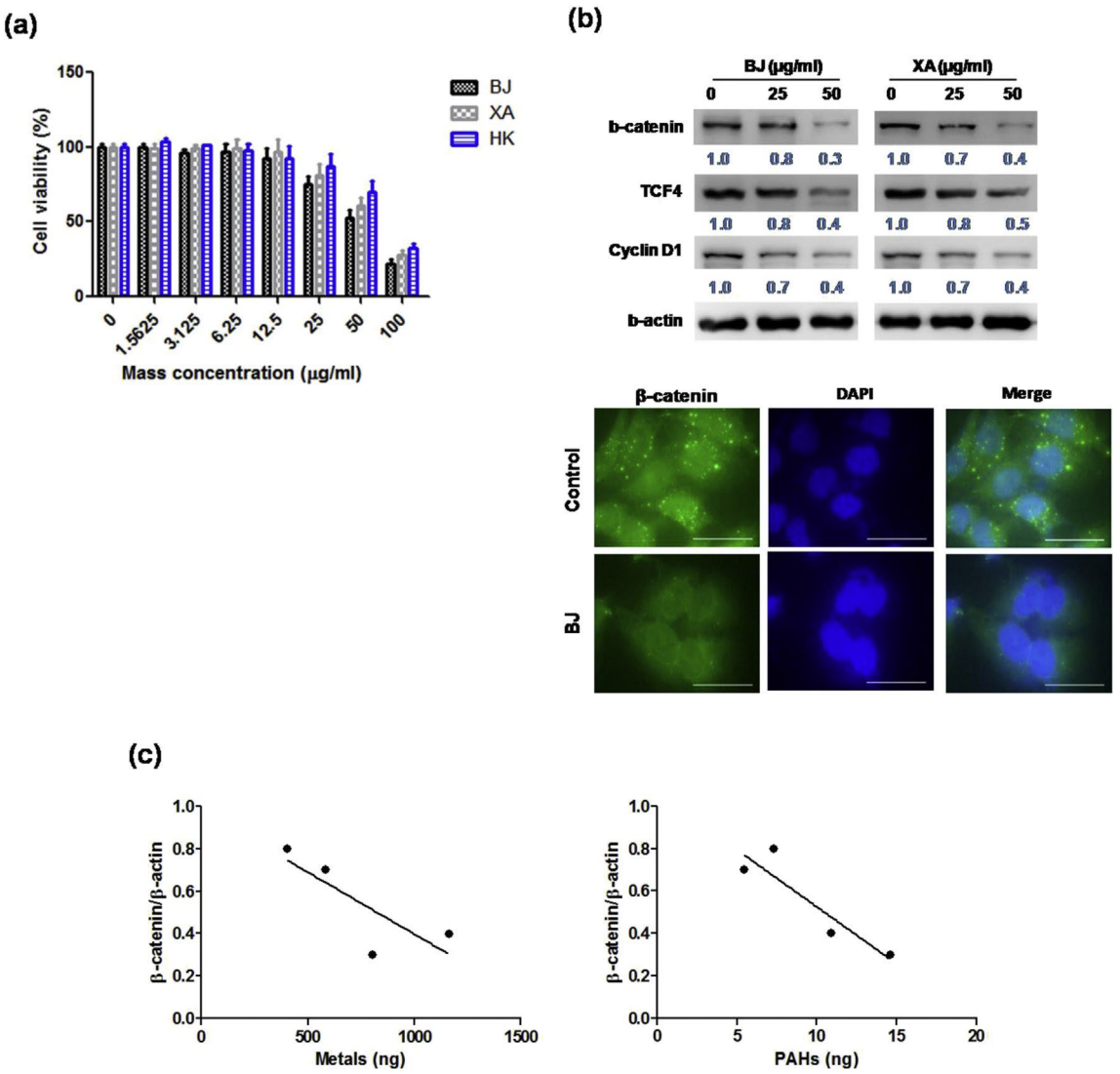

Fig. 5. (a) Effects of haze $PM_{2.5}$ (BJ, XA and HK) on the viability of A549 cells. (b) Haze $PM_{2.5}$ (BJ and XA) down-regulated the expression of β-catenin, TCF4, which has transcriptional activity, and its downstream target cyclin D1 in A549 cells. Indirect immunofluorescence analysis of β-catenin in the A549 cells post-exposure to BJ $PM_{2.5}$. Green: b-catenin staining, blue: nuclear staining by DAPI. (c) Trends of β-catenin with total metals and PAHs.

Table 1
Physicochemical characterization of $PM_{2.5}$ collected in BJ, XA and HK during a haze episode.

	BJ	XA	HK
Meteorological information			
Humidity (%)	77 ± 15	48 ± 17	73 ± 6
Visibility (m)	3353 ± 2949	2130 ± 1503	NA
Physical characterization			
Hydrodynamic diameter (nm)			
50 μg/ml	250	253	207
150 μg/ml	422	449	466
Zeta potential (mV)			
50 μg/ml	−34	−14	−17
150 μg/ml	−18	−13	−7
Metals (ng/m^3)			
Al	481.2 ± 299.7	849.2 ± 564.7	158.7 ± 11.7
Cs	29.9 ± 25.2	54.7 ± 2.8	2.8 ± 2.4
Cd	5.0 ± 3.8	5.2 ± 0.5	0.3 ± 0.2
Co	1.5 ± 0.3	1.3 ± 0.2	0.4 ± 0.1
Cu	59.9 ± 30.5	37.8 ± 5.9	41.4 ± 7.1
Fe	1171.1 ± 324.1	1033.7 ± 496.0	237.8 ± 43.9
Ni	7.0 ± 1.6	4.7 ± 1.5	5.3 ± 2.6
Pb	362.1 ± 191.6	260.4 ± 17.4	23.1 ± 14.4
V	4.7 ± 1.8	3.7 ± 2.2	12.9 ± 8.4
Zn	443.7 ± 272.4	938.2 ± 222.7	77.0 ± 33.5
Cr	12.3 ± 4.3	11.8 ± 1.8	3.9 ± 0.6
Mn	54.5 ± 34.8	59.2 ± 13.4	ND
Mo	3.0 ± 0.4	4.2 ± 0.8	0.4 ± 0.3
Se	14.5 ± 7.5	12.1 ± 1.1	2.7 ± 1.9
Sr	6.9 ± 2.5	9.3 ± 5.3	1.5 ± 0.3
Ti	18.7 ± 5.9	32.4 ± 17.9	4.1 ± 0.7
Total	**2675.9 ± 1143.5**	**3318.0 ± 1280.9**	**570.2 ± 99.3**

NA: not available.
ND: not detected.

Table 2
Correlations of β-catenin, caspase-3 activity and alveolar number with the 15 PAHs and 16 metals in the haze $PM_{2.5}$. The correlations were calculated using Pearson's correlation coefficients (*$p < 0.05$).

	β-catenin	Caspase-3 activity	Alveolar number
Metals			
Al	−0.5859	0.5981	−0.2266
Cs	−0.6723	0.7575	−0.6155
Cd	**−0.8607***	**0.9463***	**−0.8860***
Co	−0.7055	0.7054	−0.4080
Cu	−0.1893	0.1299	0.1699
Fe	−0.7963	**0.8119***	−0.5392
Ni	−0.1699	0.1095	0.1930
Pb	**−0.8893***	**0.9640***	**−0.9561***
V	−0.0311	−0.0385	0.3343
Zn	−0.6463	0.7145	−0.4757
Cr	**−0.5396***	0.5187	−0.1885
Mn	**−0.9539***	**0.9651***	−0.8581
Mo	**−0.8197***	**0.8911***	−0.6842
Se	**−0.8383***	**0.8609***	−0.6148
Sr	−0.7740	0.8099	−0.4978
Ti	−0.7124	0.7614	−0.4578
PAHs			
Naphthalene	−0.7197	**0.8144***	**−0.8743***
Acenaphthylene	−0.7175	**0.8125***	**−0.8699***
Acenaphthene	−0.7402	**0.8284***	**−0.9272***
Fluorene	−0.3931	0.3505	−0.0590
Phenanthrene	−0.7653	**0.8333***	**−0.9480***
Anthracene	−0.7578	**0.8230***	**−0.9419***
Fluoranthene	−0.7646	**0.8428***	**−0.9526***
Pyrene	−0.8041	**0.8845***	**−0.9597***
Benz(a)anthracene	−0.7657	**0.8487***	**−0.9477***
Chrysene	**−0.7910***	**0.8780***	**−0.9412***
Benzo(b+k)fluoranthene	**−0.8206***	**0.9090***	**−0.9263***
Benzo(a)pyrene	**−0.8505***	**0.9368***	**−0.9230***
Indeno(1,2,3-cd)pyrene	−0.8331	**0.9144***	−0.7713
Dibenz(a,h)anthracene	−0.5532	0.5399	−0.1870
Benzo(g,h,i)perylene	−0.7821	**0.8575***	−0.6615

REFERENCES

Cadigan, K.M., Nusse, R., 1997. Wnt signaling: a common theme in animal development. Genes. Dev. 11, 3286 - 3305.

Capaldo, C.T., Beeman, N., Hilgarth, R.S., Nava, P., Louis, N.A., Naschberger, E., et al., 2012. IFN-gamma and TNF-alpha-induced GBP-1 inhibits epithelial cell prolif- eration through suppression of beta-catenin/TCF signaling. Mucosal Immunol. 5, 681 - 690.

Chilosi, M., Poletti, V., Zamo, A., Lestani, M., Montagna, L., Piccoli, P., et al., 2003. Aberrant Wnt/beta-catenin pathway activation in idiopathic pulmonary fibrosis. Am. J. Pathol. 162, 1495 - 1502.

Chuang, H.C., Fan, C.W., Chen, K.Y., Chang-Chien, G.P., Chan, C.C., 2012. Vasoactive alteration and inflammation induced by polycyclic aromatic hydrocarbons and trace metals of vehicle exhaust particles. Toxicol. Lett. 214, 131 - 136.

Chuang, H.C., Jones, T.P., Lung, S.C., Be'ruBe', K.A., 2011a. Soot-driven reactive oxygen

species formation from incense burning. Sci. Total Environ. 409, 4781 - 4787.

Churg, A., Wright, J.L., 2002. Airway wall remodeling induced by occupational mineral dusts and air pollutant particles. Chest 122, 306S - 309S.

Emmanuel, S.C., 2000. Impact to lung health of haze from forest fires: the Singapore experience. Respirology 5, 175 - 182.

Fairbairn, E.A., Bonthius, J., Cherr, G.N., 2012. Polycyclic aromatic hydrocarbons and dibutyl phthalate disrupt dorsal-ventral axis determination via the Wnt/beta- catenin signaling pathway in zebrafish embryos. Aquat. Toxicol. 124e125, 188 - 196.

Farina, F., Sancini, G., Mantecca, P., Gallinotti, D., Camatini, M., Palestini, P., 2011. The acute toxic effects of particulate matter in mouse lung are related to size and season of collection. Toxicol. Lett. 202, 209 - 217.

Ghanem, M.M., Battelli, L.A., Mercer, R.R., Scabilloni, J.F., Kashon, M.L., Ma, J.Y., et al., 2006. Apoptosis and Bax expression are increased by coal dust in the polycyclic aromatic hydrocarbon-exposed lung. Environ. Health Perspect. 114, 1367 - 1373.

Huang, Y.C., Li, Z., Harder, S.D., Soukup, J.M., 2004. Apoptotic and inflammatory effects induced by different particles in human alveolar macrophages. Inhal.Toxicol. 16, 863 - 878.

Imoto, M., Tanabe, K., Simizu, S., Tashiro, E., Takada, M., Umezawa, K., 1998. Inhibition of cyclin D1 expression and induction of apoptosis by inostamycin in small cell lung carcinoma cells. Jpn. J. Cancer Res. 89, 315 - 322.

Institute, H.E., 2013. Outdoor Air Pollution Among Top Global Health Risk in 2010: Risks Especially High in China and Other Developing Countries of Asia.

Konigshoff, M., Eickelberg, O., 2010. WNT signaling in lung disease: a failure or a regeneration signal? Am. J. Respir. Cell. Mol. Biol. 42, 21 - 31.

Lam, A.P., Gottardi, C.J., Tuder, R., 2011. Regenerative pathways and emphysema: a new paradigm? Am. J. Respir. Crit. Care Med. 183, 688 - 690.

Lee, K.-Y., Wong, C.K.-C., Chuang, K.-J., Bien, M.-Y., Cao, J.-J., Han, Y.-M., et al., 2014. Methionine oxidation in albumin by haze fine particulate matter: an in vitro and in vivo study. J. Hazard Mater. 274, 384 - 391.

Li, V.S., Ng, S.S., Boersema, P.J., Low, T.Y., Karthaus, W.R., Gerlach, J.P., et al., 2012. Wnt signaling through inhibition of beta-catenin degradation in an intact Axin1 complex. Cell 149, 1245 - 1256.

Libalova, H., Uhlirova, K., Klema, J., Machala, M., Sram, R.J., Ciganek, M., et al., 2012. Global gene expression changes in human embryonic lung fibroblasts induced by organic extracts from respirable air particles. Part Fibre Toxicol. 9, 1.

MacDonald, B.T., Tamai, K., He, X., 2009. Wnt/beta-catenin signaling: components, mechanisms, and diseases. Dev. Cell. 17, 9 - 26.

Murray, C.J., Ortblad, K.F., Guinovart, C., Lim, S.S., Wolock, T.M., Roberts, D.A., et al., 2014. Global, regional, and national incidence and mortality for HIV, tubercu- losis, and malaria during 1990e2013: a systematic analysis for the Global Burden of Disease Study 2013. Lancet 384, 1005 - 1070.

Nelson, W.J., Nusse, R., 2004. Convergence of Wnt, beta-catenin, and cadherin pathways. Science 303, 1483 - 1487.

Steinhusen, U., Badock, V., Bauer, A., Behrens, J., Wittman-Liebold, B., Dorken, B., et al., 2000. Apoptosis-induced cleavage of beta-catenin by caspase-3 results in proteolytic fragments with reduced transactivation potential. J. Biol. Chem. 275, 16345 - 16353.

Su, C.L., Chen, T.T., Chang, C.C., Chuang, K.J., Wu, C.K., Liu, W.T., et al., 2013. Comparative proteomics of inhaled silver nanoparticles in healthy and allergen provoked mice. Int. J. Nanomedicine 8, 2783 - 2799.

Sun, Y., Taguchi, K., Sumi, D., Yamano, S., Kumagai, Y., 2006a. Inhibition of endo- thelial nitric oxide synthase activity and suppression of endothelium- dependent vasorelaxation by 1,2-naphthoquinone, a component of diesel exhaust particles. Arch. Toxicol. 80, 280 - 285.

Sun, Y., Zhuang, G., Tang, A.A., Wang, Y., An, Z., 2006b. Chemical characteristics of PM2.5 and PM10 in haze-fog episodes in Beijing. Environ. Sci. Technol. 40, 3148 - 3155.

Sun, Z., Mu, Y., Liu, Y., Shao, L., 2013. A comparison study on airborne particles during haze days and non-haze days in Beijing. Sci. Total Environ. 456e457, 1 - 8.

Thurston, G.D., Ito, K., Hayes, C.G., Bates, D.V., Lippmann, M., 1994. Respiratory hospital admissions and summertime haze air pollution in Toronto, Ontario: consideration of the role of acid aerosols. Environ. Res. 65, 271 - 290.

Tian, S., Pan, Y., Liu, Z., Wen, T., Wang, Y., 2014. Size-resolved aerosol chemical analysis of extreme haze pollution events during early 2013 in urban Beijing, China. J. Hazard Mater. 279, 452 - 460.

Vichai, V., Kirtikara, K., 2006. Sulforhodamine B colorimetric assay for cytotoxicity screening. Nat. Protoc. 1, 1112 - 1116.

Wang, R., Ahmed, J., Wang, G., Hassan, I., Strulovici-Barel, Y., Hackett, N.R., et al., 2011. Down-regulation of the canonical Wnt beta-catenin pathway in the airway epithelium of healthy smokers and smokers with COPD. PLoS One 6, 14793.

WHO, 2006. WHO Air Quality Guidelines for Particulate Matter, Ozone, Nitrogen Dioxide and Sulfur Dioxide. World Health Organization.

Wu, X., Deng, G., Hao, X., Li, Y., Zeng, J., Ma, C., et al., 2014. A caspase-dependent pathway is involved in Wnt/beta-catenin signaling promoted apoptosis in Ba- cillus Calmette-Guerin infected RAW264.7 macrophages. Int. J. Mol. Sci. 15, 5045 - 5062.

Xia, T., Korge, P., Weiss, J.N., Li, N., Venkatesen, M.I., Sioutas, C., et al., 2004. Quinones and aromatic chemical compounds in particulate matter induce mitochondrial dysfunction: implications for ultrafine particle toxicity. Environ. Health Perspect. 112, 1347 - 1358.

Xu, P., Chen, Y., Ye, X., 2013. Haze, air pollution, and health in China. Lancet 382, 2067.

Yang, K., Hitomi, M., Stacey, D.W., 2006. Variations in cyclin D1 levels through the cell cycle determine the proliferative fate of a cell. Cell. Div. 1, 32.

Zhang, Z., Wang, J., Chen, L., Chen, X., Sun, G., Zhong, N., et al., 2014. Impact of haze and air pollution-related hazards on hospital admissions in Guangzhou, China. Environ. Sci. Pollut. Res. Int. 21, 4236 - 4244.